

Resource Allocation and Computation Offloading in a Millimeter-Wave Train-Ground Network

Linqian Li, Yong Niu, *Member, IEEE*, Shiwen Mao, *Fellow, IEEE*, Bo Ai, *Senior Member, IEEE*, Zhangdui Zhong, *Senior Member, IEEE*, Ning Wang, *Member, IEEE*, and Yali Chen

Abstract—In this paper, we consider an mmWave-based train-ground communication system in the high-speed railway (HSR) scenario, where the computation tasks of users can be partially offloaded to the rail-side base station (BS) or the mobile relays (MRs) deployed on the roof of the train. The MRs operate in the full-duplex (FD) mode to achieve high spectrum utilization. We formulate the problem of minimizing the average task execution latency of all users, under local device and MRs energy consumption constraints. We propose a joint resource allocation and computation offloading scheme (JRACO) to solve the problem. It consists of a resource allocation and computation offloading (RACO) algorithm and an MR Energy constraint algorithm. RACO utilizes the matching game theory to iterate between two subproblems, i.e., data segmentation and user association and sub-channel allocation. With the RACO results, the MR energy constraint algorithm ensures that the MR energy consumption constraint is satisfied. Extensive simulations validate that JRACO can effectively reduce the average latency and increase the number of served users compared with three baseline schemes.

Index Terms—Mobile edge computing (MEC), Full-duplex (FD) communications, Millimeter-wave (mmWave) communications, Train-ground communications, Resource allocation.

I. INTRODUCTION

With the explosive growth of mobile computing applications, the 5G and beyond network systems should be able to provide differentiated services to various applications, with respect to throughput, delay, and other performance indicators. High-speed railway (HSR), as a convenient and green public transportation system, has been developed rapidly, and will become the future trend of global railway transportation in many countries. On the other hand, considering that users tend to cluster in a railway cabin and travel for long journeys, it is not inconceivable that they would be very interested in having Internet service in the train, especially in multimedia services. It is thus important to provide high quality broadband wireless access for passengers. However, the current communication technology, i.e., Global System for Mobile Communications-Railway (GSM-R), which has been widely used in high-speed railway scenarios, has many shortcomings, such as insufficient capacity, low network resource utilization, and limited data service support [1]. When the speeds of the train are over 300 km/h, the wireless channel exhibits rapidly time-varying and nonstationary features. Accordingly, even the latest generation of HSR communications systems, LTE for Rail (LTE-R), cannot provide every user with broadband services due to bandwidth limitations. The increasing demand for HSR communications leads to significant attention on the study of spectrum extension.

To this end, millimeter wave (mmWave) communications can provide transmission rates on the order of gigabits for broadband multimedia services, including high-speed data transmission between devices, high-definition TV live broadcast, and cellular access, etc. [2], [3]. However, mmWave signals experience considerably higher propagation losses than sub-6GHz signals, are unable to penetrate most solid materials, and are particularly sensitive to blockage, resulting in higher signal attenuation and reflection [4], [5].

Communication scenarios in the HSR environment mainly include intra-compartment communications and train-ground communications. In order to offer broadband services, different reliable communication systems that can provide better performance and mobility support for users can be deployed inside train cabins, such as wireless local area networks (WLAN), most modern communication devices can use this system if equipped with a WLAN network interface card [6]. In addition, mmWave communications can be leveraged for train-ground communications, where mobile relays (MRs) can be deployed on the rooftop of the train. In order to compensate for the severe attenuation of mmWave signals, directional antennas are usually used to achieve a high antenna gain.

Another relevant technology is Full-duplex (FD) transmission, which has attracted great attentions in both academia and industry. The FD technology allows wireless communication devices to transmit and receive signals simultaneously on the same frequency band by utilizing separated or shared antenna configuration. With the advances of self-interference (SI) cancellation techniques, FD communications can greatly enhance the spectrum utilization and system capacity, and has been recognized as one of the key physical layer technologies of 5G and beyond.

The biggest challenge of FD communications is the elimination of SI [9]. In order to achieve high spectral efficiency, existing schemes have been able to achieve 100dB reduction of SI through antenna separation, digital domain elimination, and analog domain elimination [8], which enables practical applications of the FD technology. Considering the HSR scenario, the MRs could adopt FD transmissions to simultaneously serve users and connect to the ground BS. How to effectively associate users to the MRs or the BS should be carefully determined. When there are many users, it is also a key problem of how to select the set of users to serve to optimize users' experience.

Recently, mobile edge computing (MEC) has emerged as a promising paradigm to support many 5G and beyond applications including latency sensitive services [10]–[12]. MEC can reduce the load on the core network and the

data transmission delay by deploying nodes with computation processing capacity at the edge of network to be closer to users. However, there has been very limited prior work on combining MEC and train-ground communication system in the HSR scenario. Utilizing mmWave communications for train-ground communications and deploying MEC servers on high-speed trains, high-speed data transmission will be enabled with the help of FD MRs, which can significantly improve the broadband wireless communication service performance of the entire train-ground communication system. The computing tasks of users can be executed locally, or be offloaded to the MRs and executed on the train, or be offloaded to the rail-side BS to be executed there.

In this paper, we investigate the problem of joint optimization of partial computation offloading, user association, and resource allocation in an mmWave FD train-ground communications system. Our objective is to minimize the average delay for all users under the energy consumption constraints of users and MRs. In particular, each user can flexibly choose to partially offload its tasks to an MR or the BS (in this case, the data transmission is still via the FD MRs). Then the MRs and the BS can cooperate with each other to execute the offloaded tasks of users by sharing their limited computing resources. The challenge is how to strike a balance between local execution and offloaded execution latencies considering dynamic data segmentation, distributed computing capacities, and FD transmissions. We formulate a mixed integer nonlinear programming (MINLP) problem and propose a low complexity heuristic algorithm, which solves the formulated problem by decomposing it into data segmentation, resource allocation problems for known user association and MR energy consumption control problem.

The main contributions made in this paper are summarized as follows.

- We propose an MEC framework for the mmWave train-ground communication system, in which MRs are deployed on the train to relay data between users and the rail-side BS and operating in the FD mode. Both the BS and MRs serve as MEC servers. Then, we formulate the problem of joint user association, partial offloading, and resource allocation, aiming to minimize the average latency by taking account of the MRs energy consumption.
- We propose a resource allocation and computation offloading (RACO) algorithm by decomposing the original problem into subproblems: the subproblem of data segmentation is solved by functional analysis, and the user association and resource allocation subproblem is solved by a matching game. In addition, a heuristic algorithm is proposed to enforce the MRs energy consumption constraint. Resource surplus and resource deficit scenarios are all considered.
- We perform extensive simulations under various system parameter settings to validate the performance of our proposed scheme and compare it with four benchmark schemes. Our results validate that the average latency of all users can be significantly reduced by the proposed scheme, while keeping the MRs' energy consumption within constraints.

The remainder of the paper is organized as follows. In Section II, we provide an overview of related work. In Section III, we introduce the train-ground communication system model, including the device, task, and partial offloading models. We discuss the formulation of average latency minimization problem in Section IV and problem decomposition in Section V. We present our proposed RACO and MRs energy constraint algorithms in Section VI. Our simulation study is presented in Section VII. Finally, Section VIII concludes this paper.

II. RELATED WORK

There has been considerable interest in FD communications in cellular networks, mmWave networks, and heterogeneous networks. Wen *et al.* [13] investigated the resource allocation and user scheduling problems to maximize network throughput in a time-division cellular network, where FD was adopted at the BS and user equipments still operate in the HD mode. To guarantee the QoS requirements of traffic flows, Ding *et al.* [14] proposed an FD scheduling algorithm in the mmWave wireless backhaul to maximize the number of completed flows. Liu *et al.* [15] proposed a novel MEC framework with a user virtualization scheme in a software-defined network virtualization cellular network, and introduced user virtualization assisted by FD communications. Lan *et al.* [16] integrated FD in an MEC enabled HetNet. A maximization optimization problem of users' revenues is formulated, in which uplink FD transmissions are considered.

For the simpler case of single-user systems, in [17], the cooperation of cloud computing and MEC was investigated in the IoT setting, and the single user computation offloading problem was solved by the branch-and-bound algorithm. Kuang *et al.* [18] investigated the joint problem of partial offloading scheduling and resource allocation with multiple independent tasks. The goal was to minimize the weighted sum of the execution delay and energy consumption, while guaranteeing the transmit power constraint of the tasks. The problem is solved by a two-level alternation method framework based on Lagrangian dual decomposition.

Other works considered the multiuser partial offloading MEC scenario. In [19], the problem of collaborative MEC offloading for multiuser multi-MEC in 5G HetNets was studied, and a game-theoretical computation offloading scheme was proposed. Mao *et al.* [20] investigated joint radio and computational resource management in the multi-user single-MEC scenario, with the objective to minimize the long-term average weighted sum power consumption of the MDs and the MEC server. An online algorithm was proposed based on Lyapunov optimization for reduced power consumption. In [21], Saleem *et al.* jointly considered partial offloading and resource allocation to minimize the sum latency with energy efficiency for multi-user MEC offloading. An expression to determine the optimal offloading fraction was derived such that energy consumed for local execution would not exceed the desired limit. Chen *et al.* [22] minimized the total energy consumption of all users within the required latency. User association was jointly considered with sub-channel allocation, which were transformed into a two-sided matching game representing the

resource competition among users. Saleem *et al.* [23] focused on minimizing the sum of task execution latency of all the devices in a shared spectrum under interference. Where desired energy consumption, partial offloading, and resource allocation constraints were considered. A decomposition approach was adopted to solve the problem, which iteratively reduced the parallel processing delay by adjusting data segmentation and solving the underlying key challenge of interference in a shared spectrum. However, the focus of the work was on interference management, and the iterative convergence speed of adjusting the unloading rate was relatively low.

As multiple users compete for the finite radio and edge computing resources, some prior works deal with resource allocation from a game-theoretic perspective. In [24], the authors modeled the network as a competitive game, where users shared the communication channel to offload their computations. Optimal offloading decision was derived for minimizing user energy consumption while satisfying the hard deadline of the applications. In [25], the problem of cloud-MEC collaborative computation offloading was investigated, and a game-theoretic collaborative computation offloading scheme was proposed. Di *et al.* [26] maximized the weighted total sum-rate by power control and sub-channel allocation, which was equivalent to a many-to-many matching game where peer effects existed.

Although great advances have been made, the problem of multiuser partial offloading in the mmWave band with FD communications has not been fully addressed in prior works so far. Meanwhile, some previous studies sought to optimize either the computation offloading strategy or computing resource allocation, but without considering both goals. Motivated by the related works, we propose to jointly optimize computation offloading and resource allocation, by modeling the sub-channel allocation problem as a matching game. In addition, different from the previous works, we consider two offloading locations, namely on the MR side and the BS side, while they communicate with each other in the FD mode and cooperate with each other to complete users' computing tasks. This paper also considers the constraints on the user energy consumption and the edge server on the MR when minimizing the system latency, which has not been fully studied in prior works.

III. SYSTEM OVERVIEW

A. System Model

We consider an mmWave-based train-ground communication system using FD MRs to serve multiple users, as shown in Fig. 1. There are one track-side BS and multiple MRs deployed on the train. The BS is installed with an MEC server and connects to the core network. The MRs operate in the FD mode and connect to users and the BS via wireless mmWave links. Thus, the computing tasks of users can be offloaded to the MRs to be completed by the server on the train, or to be offloaded to the BS by the MRs. We do not consider the case where users are directly connected to the track-side BS, because users are often closer to the MRs in practical scenarios. In addition, the propagation of mmWave signals is

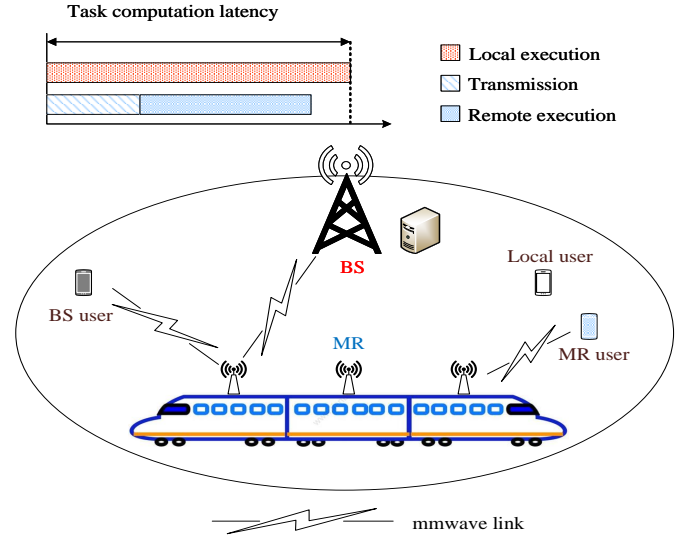


Fig. 1. Illustration of the mmWave train-ground communication system.

highly vulnerable to various blockages (e.g., the cabin wall or glass window) due to its weak diffraction capability. Thus, it is inappropriate for users to directly associate with the BS. All the devices in this system work in the mmWave band. The BS and MRs are all equipped with steerable directional antennas to achieve a high antenna gain.

We assume that the equal bandwidth resources allocated to the MRs are mutually independent. At each MR, multiple sub-channels are equally partitioned based on the available channel bandwidth. Different sub-channels adopt orthogonal frequency division and each sub-channel can serve at most one user. Based on the above assumptions, there is no co-channel interference between users. We assume that each user is aware of the location of the neighboring MR, as well as its own location. The user will establish an association with the closest MR. Each MR has S independent sub-channels of equal bandwidth, denoted by $\mathbf{S} = \{1, 2, \dots, S\}$.

Assume that there are M users under the coverage of an MR. The corresponding set of users is denoted as $\mathbf{M} = \{1, 2, \dots, M\}$. Users that can ultimately perform task offloading are divided into two categories, namely, BS users and MR users. Specifically, the user set associated with an MR is denoted as \mathcal{U}^R , and the user set connected to BS is denoted as \mathcal{U}^B . The devices in the set have limited computation resources but need to perform a delay-sensitive and computation-intensive task. Specifically, we focus on applications with partitionable data, in which the amount of data to be processed is known beforehand and the execution can be in parallel. That is, the application data can be partitioned into subsets of any size. In practice, many mobile applications are composed of multiple procedures, making it possible to implement partial offloading. We consider the case where each user has only one task to offload, and characterize the task of user $m \in \mathbf{M}$ with two key parameters (d_m, c_m) , where d_m is the data size of the task in bits, and c_m is the computation resource required to process one data bit in CPU cycles per bit. The quasistatic scenario is considered in this paper, where the set of

TABLE I
NOTATION

| Notation | Description |
|-----------------|---|
| \mathbf{M} | the set of users |
| \mathbf{S} | the set of sub-channels |
| \mathbf{Y}_m | the remotely executed portion set of user m |
| \mathcal{U}^R | the set of MR users |
| \mathcal{U}^B | the set of BS users |
| d_m | the task data size of user m |
| c_m | the task processing density of user m |
| λ_m | the local execution fraction of user m |
| E_m | the energy constraint of user m |
| E^R | the energy constraint of the MRs |
| $x_{m,s}$ | whether sub-channel s is occupied by user m |
| W | the subcarrier bandwidth |
| β | the SI cancellation level of the MRs |
| f_m^R, f_m^B | the computation resource allocation of an MR, BS |
| P_m^R | the transmit power of the MR assigned to user m |

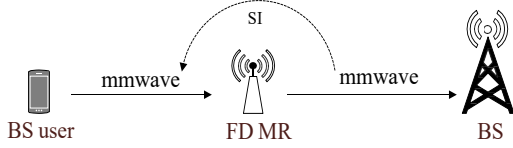


Fig. 2. Illustration of the self-interference (SI) at an FD MR.

users remains unchanged during an offloading period. Table I summarizes the main notation used in this paper.

B. Partial Offloading Model

We consider the partial offloading model, motivated by the fact that it benefits from parallel computing by efficiently utilizing the local and remote resources simultaneously [30]. In particular, we adopt a data-partition model, where the input bits of the task can be arbitrarily divided due to bit-wise independence [31]. Under this model, a fraction of the task can be processed locally, and the rest can be offloaded to the MR or BS. We introduce the parameter $\lambda_m \in [0, 1]$ to represent the ratio of the locally executed portion of user m 's task. After determining the partitioning of task data, $\lambda_m d_m$ bits will be processed locally, while $(1 - \lambda_m)d_m$ bits will be offloaded to either the BS or MR. For ease of notation, the set of binary variables \mathbf{Y}_m representing the remote execution locations is introduced and defined as $\mathbf{Y}_m = \{(y_m^R, y_m^B) | m \in \mathbf{M}\}$, where $y_m^R = 1$ indicates that user m offloads task to the MR, and $y_m^B = 1$ indicates that user m offloads task to the BS.

For a user, offloading tasks to the MR or BS are different in the wireless transmission rate, because offloading tasks to the BS still requires the help of MR, which works in the FD communication mode to relay the user's computing tasks to the BS. Since data is received and transmitted simultaneously in the FD mode, self-interference (SI) is introduced at the MR, as shown in Fig. 2, which needs to be considered.

The execution of a user task involves local execution, BS execution, and MR execution, which are modeled in the following.

1) *Local Execution:* We denote f_m^L as the CPU speed of completing locally executed tasks for user m , which is measured by the amount of CPU cycles per second. The advanced dynamic frequency and voltage scaling (DFVS) technique is adopted, which allows stepping-up or -down of the CPU cycle frequency. In practice, the value of f_m^L is bounded by a maximum value f_m^{max} , which is due to the limitation of the user's computation capability. The user will process a fraction of its task locally, whereas the time consumption of local computation depends on the CPU clock frequency f_m^L , the data size of the task d_m , and the number of CPU cycles required per bit c_m . Then the local computation latency t_m^L is given by

$$t_m^L = \frac{\lambda_m d_m c_m}{f_m^L}. \quad (1)$$

We model the local CPU power consumption by $\mu(f_m^L)^3$ as in [11] [30], where μ is a coefficient depending on the chip architecture. The local energy consumption for user m is shown as follows.

$$E_m^L = \mu(f_m^L)^3 t_m^L = \mu \lambda_m d_m c_m (f_m^L)^2. \quad (2)$$

2) *MR Execution:* If the remote execution location of user m is chosen to be the nearest MR, we need to determine firstly which sub-channel of this MR to access for offloading. For ease of notation, the binary variable $x_{m,s}$ is defined, where $x_{m,s} = 1$ indicates that user m occupies sub-channel s . Given the allocated spectrum resources, the signal to interference plus noise ratio (SINR) of user m connected to MR through sub-channel s can be expressed as

$$\Gamma_{m,s}^R = \frac{H_s G_t(m, R, s) G_r(m, R, s) l_{mR}^{-\alpha} P_m}{N_0 W}, \quad (3)$$

where H_s is the gain of sub-channel s following the Nakagami- m_s distribution with parameters $\{m_s, w_s\}$, where m_s is the fading depth parameter and w_s is the average power in the fading signal [22]; $G_t(m, R, s)$ and $G_r(m, R, s)$ are the transmitting gain and receiving gain of the directional antenna pointing from user m to the MR on sub-channel s , respectively; $l_{mR}^{-\alpha}$ is the path loss of link m to the MR with path loss exponent α ; P_m is the transmit power of user m (to simplify analysis, we consider constant transmit power); N_0 is the white Gaussian noise power spectral density; and W is the subcarrier bandwidth depending on channel bandwidth and the number of sub-channels partitioned. According to the Shannon theory, the achievable transmission rate is

$$R_{m,s}^R = W \log_2(1 + \Gamma_{m,s}^R). \quad (4)$$

Thus, the time consumed to upload $(1 - \lambda_m)d_m$ data bits to the MR is

$$t_m^R = \frac{(1 - \lambda_m)d_m}{R_{m,s}^R}, \quad (5)$$

and the transmission energy consumption of user m can be expressed as

$$E_m^R = P_m t_m^R. \quad (6)$$

When task offloading is completed, the edge server computing process begins. We suppose the processing speed of the MR as f_m^R in CPU cycles per second for serving user m . The MR's remote execution latency for user m is given by

$$t_m^{eR} = \frac{(1 - \lambda_m)d_m c_m}{f_m^R}. \quad (7)$$

Since the size of the remote execution results to the users are extremely small, this part of time and energy costs can be neglected. Similar to (2), the energy consumption of the MR to complete the task of user m is

$$E_m^{eR} = \xi(f_m^R)^3 t_m^{eR} = \xi(1 - \lambda_m)d_m c_m (f_m^R)^2. \quad (8)$$

As we assume finite computation capacity at the MR, a feasible computation resource allocation at the MR should satisfy $\sum_{m=1}^M \sum_{s=1}^S x_{ms} y_m^R f_m^R \leq f^R$, where f^R is the total computation capacity of the MR in CPU cycles per second.

3) *BS Execution*: If the remote execution location of user m is chosen to be the BS, we have $y_m^B = 1$. Since the offloaded data will still be forwarded by the MR, we call the transmission of computing tasks from user m to MR and from MR to the BS as the first hop and the second hop, respectively. It should be noted that, because the MR operates in the FD mode, the task transfers on the first hop and the second hop are in parallel. The MR receives data from user m while forwarding data to the BS at the same time on the same sub-channel. The signal of the first hop will suffer from the background noise as well as SI due to imperfect SI cancellation. The specific cancellation methods are out of the scope of the paper, the value of residual SI after cancellation can be expressed in terms of the transmit power to facilitate the calculation. Specifically, we use βP_m^R to represent the residual SI, where β is the SI cancelation level of the MR, which is a non-negative parameter, and P_m^R is the transmit power of the MR serving user m . The first hop SINR of user m connected to the MR through sub-channel s can be expressed as

$$\Gamma_{ms}^{B1} = \frac{H_s G_t(m, R, s) G_r(m, R, s) l_{mR}^{-\alpha} P_m^R}{N_0 W + \beta P_m^R}. \quad (9)$$

The numerator of Γ_{ms}^{B1} is exactly the same as the numerator of (3), except that we have the residual SI in the denominator. The achievable transmission rate of the first hop according to the Shannon formula is

$$R_{ms}^{B1} = W \log_2(1 + \Gamma_{ms}^{B1}). \quad (10)$$

Similar to (3), the SINR of the second hop from MR to the BS can be presented as

$$\Gamma_{ms}^{B2} = \frac{H_s G_t(R, B, s) G_r(R, B, s) l_{RB}^{-\alpha} P_m^R}{N_0 W}, \quad (11)$$

where $G_t(R, B, s)$ and $G_r(R, B, s)$ are the transmitting gain and receiving gain of the directional antenna pointing from the MR to the BS on sub-channel s , respectively; $l_{RB}^{-\alpha}$ is the path loss of the MR-BS link with path loss exponent α ; and P_m^R is the transmit power of the MR assigned to user m .

Similarly, the data rate of the second hop from the MR to the BS can be computed as

$$R_{ms}^{B2} = W \log_2(1 + \Gamma_{ms}^{B2}). \quad (12)$$

According to [33], the available data rate depends on the smaller of the first and second hop data rates as

$$R_{ms}^B = \min\{R_{ms}^{B1}, R_{ms}^{B2}\}. \quad (13)$$

Thus, the transmission delay consumed to upload $(1 - \lambda_m)d_m$ data bits to the BS can be written as

$$t_m^B = \frac{(1 - \lambda_m)d_m}{R_{ms}^B}. \quad (14)$$

And the transmission energy consumption of user m can be expressed as

$$E_m^B = P_m t_m^B. \quad (15)$$

Whereas, the transmission energy consumption of the MR can be expressed in terms of the transmit power of the MR assigned to user m , as well as the transmission time as

$$E_m^{tR} = P_m^R t_m^B. \quad (16)$$

Denote f_m^B as the processing speed of the BS in CPU cycles per second for serving user m . The BS's remote execution latency for user m is given by

$$t_m^{eB} = \frac{(1 - \lambda_m)d_m c_m}{f_m^B}. \quad (17)$$

Similarly, we also assume the total computing capacity of the BS is limited by f^B in CPU cycles per second, as $\sum_{m=1}^M \sum_{s=1}^S x_{ms} y_m^B f_m^B \leq f^B$, where f^B is the total computation capacity of the BS in CPU cycles per second.

Hitherto we have described the train-ground communication mmWave based MEC system and presented the partial offloading model consisting of three cases: local execution, MR execution, and BS execution. We proceed to formulate the joint user association, data segmentation, and resource allocation problem in the next section with the goal of minimizing all the users' latency.

IV. PROBLEM FORMULATION

We aim to minimize the average task execution latency of all users, which can partially offload their computation tasks to the BS or the MRs. Once all users have determined the amount of data to be offloaded and the target execution locations, the portion of the data for remote execution is transferred over the wireless link to the associated BS or MR. When the transmission is completed, the task will be executed by the remote server at the corresponding location. For partial offloading, there are two processes involved, namely local computation and task offloading (i.e., uploading task data and remote execution). Since local computation can be executed in parallel with the computation offloading process, the total task computation delay for a user m is determined by the longer process, given by

$$t_m = \max\{t_m^L, x_{ms} y_m^R (t_m^R + t_m^{eR}), x_{ms} y_m^B (t_m^B + t_m^{eB})\}. \quad (18)$$

With the system model in Section III, we formulate a joint partial offloading, communication and computation resource allocation problem as follows.

$$\mathbf{P1} : \min_{\lambda, \mathbf{x}, \mathbf{Y}, \mathbf{f}, \mathbf{P}^R} \bar{t} = \frac{1}{M} \sum_{m=1}^M t_m, \forall m \in M \quad (19a)$$

$$\begin{aligned}
\text{s.t. } 0 &\leq \lambda_m \leq 1 & (19b) \\
y_m^R, y_m^B &\in \{0, 1\}, \forall m \in \mathbf{M} & (19c) \\
y_m^R = 1 \text{ or } y_m^B &= 1, \text{ if } \lambda_m \neq 1 & (19d) \\
y_m^R + y_m^B &\leq 1 & (19e) \\
x_{ms} &\in \{0, 1\}, \forall m \in \mathbf{M}, s \in \mathbf{S} & (19f) \\
\sum_{s=1}^S x_{ms} &\leq 1, \forall m \in \mathbf{M} & (19g) \\
\sum_{m=1}^M \sum_{s=1}^S x_{ms} &\leq S & (19h) \\
y_m^R (E_m^L + E_m^R) &\leq E_m, \forall m \in \mathbf{M} & (19i) \\
y_m^B (E_m^L + E_m^B) &\leq E_m, \forall m \in \mathbf{M} & (19j) \\
0 \leq f_m^L &\leq f_m^{\max} & (19k) \\
\sum_{m=1}^M \sum_{s=1}^S x_{ms} y_m^R f_m^R &\leq f^R & (19l) \\
\sum_{m=1}^M \sum_{s=1}^S x_{ms} y_m^B f_m^B &\leq f^B & (19m) \\
\sum_{m=1}^M \sum_{s=1}^S x_{ms} (y_m^R E_m^{eR} + y_m^B E_m^{tR}) &\leq E^R. & (19n)
\end{aligned}$$

Constraint (19b) specifies the range of the data portion that can be executed locally when user m performs a partial offloading. The constraints relating to user association are presented in (19c)-(19e). Specifically, (19d) explains that a certain number of tasks will be offloaded when the user establishes an association with the BS or an MR, whereas (19e) indicates that the user chooses one of the MRs or the BS as the remote execution location. Constraints (19f)-(19h) are based on the fact that spectrum resources are limited. Specifically, (19g) ensures that a user can be assigned with at most one sub-channel of the MR. Constraint (19h) indicates that the total number of sub-channels assigned to users are limited by the total number of available sub-channels. Constraints (19i) and (19j) ensure that the energy consumption of the computation offloading process of user m , which consists of local computing and transmission energy consumption, cannot exceed the local energy budget E_m . Constraint (19k) is on the local CPU processing capability budget. Constraints (19l) and (19m) ensure feasible computation resource allocation at the MR and the BS, respectively. Finally, constraint (19n) indicates that the execution energy consumption and transmission energy consumption consumed by an MR are limited by E^R (i.e. The total energy of MR).

There is no doubt that the formulated average latency minimization problem is a mixed-integer nonlinear and non-convex programming problem. Furthermore, the coupling of integer and continuous variables results in nonlinear constraints and non-convex feasible region. In terms of complexity, the formulated problem is NP-hard, and is hard to solve in polynomial time. Therefore, we shall propose an efficient and practical solution algorithm in the next sections.

V. PROBLEM DECOMPOSITION

It can be seen that if the user association is determined, constraints (19b) and (19i)-(19k) can be decoupled from the communication and computation resource allocation constraints (19h) and (19l)-(19m). This implies that the problem can be solved by decomposition. For known user association, we first decide the data segmentation policy considering the energy and local CPU processing capability constraints (19i)-(19k). Then, the original problem is transformed into a resource allocation problem under the energy consumption constraint of MRs and computation resource constraints of MRs and the BS.

A. Data Segmentation Policy

An important question for partial offloading is how to determine the optimal partition of data offloaded by a user, as it affects both the time consumption for local execution, offloading and remote execution, and the energy consumption for local computing and offloading. Based on constraint (19i)-(19k), an energy efficient and local computation frequency bounded data segmentation policy can be derived.

Observing the objective function (19a) and (18), we can see that the minimum latency for a user m is reached when the two parallel processes (i.e., local execution and offloading plus remote execution) take the same amount of time. However, it is uncertain whether the user can equalize the time consumption of these two processes under various constraints. We first examine the upper bound and lower bound of the offloading fraction. Assuming that the association relationship of user m has been established, then the original problem **P1** can be transformed into the following problem.

$$\begin{aligned}
\mathbf{P2} : \min_{\lambda_m, f_m^L} \bar{t} &= \frac{1}{M} \sum_{m=1}^M t_m & (20) \\
\text{s.t. Constraints } &(19b), (19i) \sim (19k).
\end{aligned}$$

If $y_m^R = 1$, i.e., user m is associated with an MR, substituting (2) and (6) into the offloading energy consumption constraints (19i), we obtain an inequality related to λ_m as

$$\mu \lambda_m d_m c_m (f_m^L)^2 + P_m \frac{(1 - \lambda_m) d_m}{R_{ms}^R} \leq E_m. \quad (21)$$

Constraint (21) serves as the feasibility condition in terms of an upper bound on λ_m , which can be easily obtained as

$$\lambda_m \leq \frac{E_m R_{ms}^R - P_m d_m}{\mu d_m c_m (f_m^L)^2 R_{ms}^R - P_m d_m}. \quad (22)$$

As stated before, λ_m is the fraction of data for local computation of user m , which satisfies $0 \leq \lambda_m \leq 1$. We next obtain an exact upper bound of λ_m as

$$\lambda_m^{\max 1} = \min \left\{ 1, \frac{E_m R_{ms}^R - P_m d_m}{\mu d_m c_m (f_m^L)^2 R_{ms}^R - P_m d_m} \right\}. \quad (23)$$

The above analysis also applies to the case where user m is associated with the BS (i.e., when $y_m^B = 1$). Similarly,

substituting (2) and (16) into constraints (19j), the exact upper bound of λ_m in this case can be obtained as

$$\lambda_m^{max2} = \min \left\{ 1, \frac{E_m R_{ms}^B - P_m d_m}{\mu d_m c_m (f_m^L)^2 R_{ms}^B - P_m d_m} \right\}. \quad (24)$$

Based on the above analysis, we obtain the feasible set of λ_m , which contains the optimal solution of problem **P2**. First, we rewrite (20) as

$$\min_{\lambda_m, f_m^L} t_m \rightarrow \min_{f_m^L} \min_{\lambda_m} t_m. \quad (25)$$

There are two independent variables in the objective function of problem **P2**. We first take one of the variables f_m^L as a constant value, and then t_m becomes a function of λ_m . Thus we can easily obtain the optimal solution λ_m , which minimizes t_m . Secondly, we substitute the optimal λ_m into t_m , where t_m only depends on f_m^L , and find the value that minimizes t_m under constraint (19k).

We still focus on the case where the user is associated with an MR as an example. When user m is associated with an MR, t_m can be written as $\max\{t_m^L, t_m^R + t_m^{eR}\}$. Observing (1), (5), and (7), for a fixed f_m^L , t_m^L is a monotonically increasing function of λ_m , while $t_m^R + t_m^{eR}$ is monotonically decreasing with λ_m . Thus the λ_m that minimizes t_m shall be obtained when $t_m^L = t_m^R + t_m^{eR}$.

$$\lambda_m^* = \frac{f_m^L (f_m^R + c_m R_{ms}^R)}{f_m^L (f_m^R + c_m R_{ms}^R) + c_m R_{ms}^R f_m^R}. \quad (26)$$

Here λ_m^* is the value that makes the time of local execution and the time of MR execution equal. It's apparent from (26) that $0 \leq \lambda_m^* \leq 1$. Combining (26) and (23) where the possible values of λ_m is given, we obtain the optimal λ_m as

$$\lambda_m^R = \begin{cases} \lambda_m^*, & \text{if } \lambda_m^* \leq \lambda_m^{max1} \\ \lambda_m^{max1}, & \text{if } \lambda_m^* > \lambda_m^{max1}. \end{cases} \quad (27)$$

Obviously, when $\lambda_m^* \leq \lambda_m^{max1}$, we choose the optimal λ_m to be λ_m^* . However, if $\lambda_m^* > \lambda_m^{max1}$, λ_m^* is out of the feasible range of λ_m . As stated before, with increased λ_m , t_m^L will increase while $t_m^R + t_m^{eR}$ will decrease. We should make these two values as close as possible to minimize t_m . Consequently, the upper bound λ_m^{max1} will be taken for λ_m .

Similarly, we can obtain the optimal λ_m when user m is associated with the BS as follows.

$$\lambda_m^B = \begin{cases} \lambda_m^*, & \text{if } \lambda_m^* \leq \lambda_m^{max2} \\ \lambda_m^{max2}, & \text{if } \lambda_m^* > \lambda_m^{max2}, \end{cases} \quad (28)$$

where λ_m^* is given by

$$\lambda_m^* = \frac{f_m^L (f_m^B + c_m R_{ms}^B)}{f_m^L (f_m^B + c_m R_{ms}^B) + c_m R_{ms}^B f_m^B}. \quad (29)$$

Note that the optimal λ_m s in (27) and (28) still contain the unknown f_m^L . For given optimal λ_m , the higher the local computing frequency f_m^L , the smaller the t_m^L , while the change in f_m^L does not affect the time it takes to complete the offloaded portion of the task. Accordingly, to some extent, a higher f_m^L can reduce t_m , and we take the optimal value of f_m^L to be the largest value in (19k) as $f_m^L = f_m^{max}$. In addition, considering that some user's task is only executed locally,

if the user's energy consumption constraint cannot support the user to complete the local computing tasks at f_m^{max} , the frequency needs to be reduced according to (2). Hence, the optimal value of f_m^L is given by

$$f_m^{*L} = \begin{cases} f_m^{max}, & \text{if } f_m^{max} \leq \sqrt{\frac{E_m}{\mu \lambda_m d_m c_m}} \\ \sqrt{\frac{E_m}{\mu \lambda_m d_m c_m}}, & \text{if } f_m^{max} > \sqrt{\frac{E_m}{\mu \lambda_m d_m c_m}}. \end{cases} \quad (30)$$

B. Power Allocation of MR

When a user offloads its tasks to the BS, due to the self-interference, the transmit power of the second hop link allocated to the MR will cause interference to the reception of the first hop link, which will greatly affect the transmission rate of the offloaded task and further affect the user's delay. The power allocation scheme for the MRs is developed in this section.

According to the SINRs and transmission rates of the first and second hop links, as well as the fact that the actual transmission rate from the user to BS depends on the smaller one of the first and second hop links, we know that when the value of P_m^R equalizes the rates of the two hops, it can minimize the time consumption for offloading and remote execution. The optimal P_m^R for user m allocated by the MR is reached when the transmission rate of the two hops take the same value and given by

$$P_m^{\text{opt}R} = \frac{-N_0 W}{2\beta} + \frac{\sqrt{(N_0 W)^2 b^2 + 4\beta N_0 W a b}}{2\beta b}, \quad (31)$$

where $a = H_s G_t(m, R, s) G_r(m, R, s) l_{mR}^{-\alpha} P_m$ and $b = H_s G_t'(m, R, s) G_r(m, B, s) l_{RB}^{-\alpha}$.

C. Communication and Computation Resource Allocation

With a given user association and data segmentation strategy, we can transform the original problem **P1** as follows for solving the communication and computing resource allocation problem, as

$$\mathbf{P3} : \min_{\mathbf{Y}_m, x_{ms}, f_m^R, f_m^B} \bar{t} = \frac{1}{M} \sum_{m=1}^M t_m \quad (32)$$

s.t. Constraints (19c) ~ (19h), (19l) ~ (19n).

Problem **P3** is still non-convex due to the product of integer and real valued variables. We simplify the computation resource allocation constraint for remote execution as follows. For the users offloading tasks to the MR, we adopt the uniform resource allocation and obtain the computation resource allocated to a user at the MR as $f_m^R = f_R / |\mathcal{U}^R|$. Similarly, each user associated with BS obtain the computing resources as $f_m^B = f_B / |\mathcal{U}^B|$.

Solving the resource allocation problem will determine whether to associate with the BS or an MR, and how the sub-channels are accessed. We denote the available resources as $\mathbf{A} = \{k | k = (\mathbf{Y}_m, s), s \in \mathbf{S}\}$, with $|\mathbf{A}| = 2 \times S$. The dual selection of users and resources can be regarded as a matching problem, i.e., modeled as a two-sided matching game. To maximize their own benefits, the users in set \mathbf{M} are matched

independently and rationally to the resources in set \mathbf{A} . Assume that the MR has perfect knowledge of the channel state information (CSI) of all users, and makes communication resources allocation decisions using such information. If $x_{ms} = 1$ and $\mathbf{Y}_m = (1, 0)$ or $(0, 1)$, we have $x_{mk} = 1$ and user m and communication resource k are matched with each other (i.e., a matched pair (m, k) is formed).

Definition 1. Given two sets $\mathbf{M} = \{1, 2, \dots, M\}$ and $\mathbf{A} = \{k | k = (\mathbf{Y}_m, s), s \in \mathbf{S}\}$, the user-resource matching state Φ is a mapping from $m \in \mathbf{M}$ to $k \in \mathbf{A}$ and from $k \in \mathbf{A}$ to $m \in \mathbf{M}$. That is to say, it holds all established matching pairs. Following are the details.

- 1) $\Phi(m) \in \mathbf{A}, \forall m \in \mathbf{M}$
- 2) $\Phi(k) \in \mathbf{M}, \forall k \in \mathbf{A}$
- 3) $|\Phi(m)| \leq 1$
- 4) $|\Phi(k)| \leq 1$
- 5) $k \in \Phi(m) \Leftrightarrow m \in \Phi(k)$.

The above definition shows that the relationship between users and resources is one-to-one if partial offloading is performed. In the case when all the tasks are executed locally, the sub-channels will be idle and no matched pair is found. The criteria for establishing matched pairs are based on the mutual preferences of both users and resources. Users are more inclined to choose resources that make their own parallel computing delay t_m smaller. Each user maintains a preference list of resources in the descending order.

Definition 2. For $k, k' \in \mathbf{A}, k \neq k'$, if $\Phi(m) = k, \Phi'(m) = k'$ (i.e., Φ and Φ' are two matched pairs), we have

$$(k, \Phi) \prec_m (k', \Phi') \Leftrightarrow t_m(k, \Phi) < t_m(k', \Phi').$$

A resource element prefers to select the user that can contribute to minimizing the total delay of all served users (including both the MR users and BS users). The preference order for resource $k \in \mathbf{A}$ can be defined as follows.

Definition 3. For $m, m' \in \mathbf{M}, m \neq m'$, if $\Phi(k) = m, \Phi'(k) = m'$, and $k = (\mathbf{Y}_m, s)$, we have

$$(m, \Phi) \prec_k (m', \Phi') \Leftrightarrow \sum_{s=1}^S x_{ms} t_m(\Phi) < \sum_{s=1}^S x_{m's} t_m(\Phi').$$

The change of the matched pair of one user will have an effect on the total delay of all served users. Under the energy consumption constraints of the MR, we define the concept of swap-matching, which help to further reduce the latency of all users, as well as the concept of swap-blocking pair in the following.

Definition 4. Given a matching Φ with $\Phi(m) = k, \Phi(k) = m, \Phi(m') = k'$, and $\Phi(k') = m'$, if a swap-matching occurs, that is, $\Phi_{mk}^{m'k'} = \Phi \setminus \{(m, k), (m', k')\} \cup \{(m, k'), (m', k)\}$, the matching pairs should be updated to $\Phi(m) = k', \Phi(k') = m, \Phi(m') = k, \Phi(k) = m'$.

Definition 5. For a pair (m, m') with $\Phi(m) = k, \Phi(k) = m, \Phi(m') = k',$ and $\Phi(k') = m'$, if the following conditions are satisfied

- 1) $(m, \Phi_{mk}^{m'k'}) \prec_{k'} (m', \Phi),$

- 2) $(m', \Phi_{mk}^{m'k'}) \prec_k (m, \Phi)$
- 3) $(k, \Phi_{mk}^{m'k'}) \prec_{m'} (k', \Phi)$
- 4) $(k', \Phi_{mk}^{m'k'}) \prec_m (k, \Phi),$

then (m, m') forms a swap-blocking pair, which means that if m and m' swap their matching resources with each other, both users and resources will be more satisfied. Taking 1) and 3) as an example, resource k' prefers to match user m rather than m' , and user m' prefers to match resource k rather than k' .

VI. THE PROPOSED JRACO SCHEME

In this section, we present the proposed joint resource allocation and computational offloading scheme (JRACO) with MR energy consumption constrained. JRACO mainly comprises two parts. The first part deals with the joint problem of communication and computing resource allocation and computing offloading aiming to minimize the delay of all users, without considering the MR energy consumption constraints in 19n. The result of the first part is then used as input to the second part, which consists of the relevant measures to control the energy consumption under the MR energy constraint (i.e. E^R).

A. Resource Allocation and Computation Offloading Algorithm

Due to limited communication resources, we should first establish a criterion to screen out those users who can be served with computational offloading. As described above, there is a certain connection between an MR link and an FD-BS link, and a sub-channel can only be assigned to one MR link or one FD-BS link. In order to simplify the analysis of selecting service users, we assume that the users being served are first associated with the MR. After determining which users can be served, we then design an association scheme for each user.

The proposed RACO algorithm is presented in Algorithm 1. If there is no reasonable admission control, the initial parameter setting could be infeasible. we assume that all users are performing on the local platform in the initial state, i.e., $\lambda_m = 1$, for all $m \in \mathbf{M}$. The parameter num_ac records the usage of resources. And the set M' records the users in descending order of d_m . Users with heavy computing tasks have priority in choosing communication resources. Steps 3-10 are for the case when there are sufficient sub-channels and Steps 12-15 are for the case when the sub-channel resource is deficit. If there is sufficient resources, users will choose the available sub-channel with the maximum transmission rate as given in Step 3. Specifically, if the number of users is less than the number of sub-channels, then the users are directly matched with the sub-channels and MRs; Otherwise, the degree of demand for resources will be evaluated. If the latency of fully edge computing is greater than that of fully MR computing for user m , sub-channel s will be occupied by user m and the matched pair (m, k) will be approved. Note that the CPU frequency of the MR here is given by $2f^R/S$. Since the final number of MR users is not yet known, we assume that the sub-channels are equally assigned to MR users

Algorithm 1 The Resource Allocation and Computation Offloading (RACO) Algorithm

Initialization: $\lambda_m = 1, \mathbf{Y}_m = (y_m^R, y_m^B) = (0, 0), x_{ms} = 0, \forall m \in \mathcal{M}, s \in \mathcal{S}, \Phi = \emptyset, num_ac = 0$

Output: $\lambda_m, f_m^R, f_m^B, x_{ms}, \forall m \in \mathcal{M}, \mathcal{U}^R, \mathcal{U}^B$

- 1: $\mathbf{S}' = \mathcal{S}, \mathbf{M}' = \text{User set in descending order of } d_m$;
- 2: **for** $m \in \mathbf{M}'$ **do**
- 3: Find $s = \text{argmax}_s R_{ms}^R, s \in \mathbf{S}'$;
- 4: **if** $M \leq S$ **then**
- 5: $x_{ms} = 1, \mathbf{Y}_m = (1, 0), \mathbf{S}' = \mathbf{S}' \setminus s, \Phi = \Phi \cup (m, k)$;
- 6: **else**
- 7: **if** $num_ac < S$ **then**
- 8: **if** $\frac{d_m c_m}{f_m^L} > \frac{d_m}{f_m^R} + \frac{d_m c_m}{f_m^R}, \text{ where } f_m^R = \frac{f^R}{S/2}$ **then**
- 9: $x_{ms} = 1, \mathbf{Y}_m = (1, 0), \mathbf{S}' = \mathbf{S}' \setminus s, \Phi = \Phi \cup (m, k), num_ac = num_ac + 1$;
- 10: **end if**
- 11: **else**
- 12: $s = \text{argmax}_s R_{ms}^R, s \in \mathcal{S}, \text{ and find } m_1 \text{ where } x_{m_1 s} = 1$;
- 13: **if** $\frac{d_m c_m}{f_m^L} - (\frac{d_m}{f_m^R} + \frac{d_m c_m}{f_m^R}) > \frac{d_{m_1} c_{m_1}}{f_{m_1}^L} - (\frac{d_{m_1}}{f_{m_1}^R} + \frac{d_{m_1} c_{m_1}}{f_{m_1}^R})$ **then**
- 14: $x_{ms} = 1, x_{m_1 s} = 0, \mathbf{Y}_m = (1, 0), \mathbf{Y}_{m_1} = (0, 0), \Phi = \Phi \setminus (m_1, k) \cup (m, k)$;
- 15: **end if**
- 16: **end if**
- 17: **end if**
- 18: **end for**
- 19: All users accessing resources are recorded in set \mathcal{U}^R ;
- 20: **repeat**
- 21: Calculate $t_m(\lambda_m^{optR}, f_m^{opt})$ for $m \in \mathcal{U}^R$;
- 22: **for** $m \in \mathcal{U}^R$ **do**
- 23: **for** $m' \in \mathcal{U}^R$ **do**
- 24: **if** $m \neq m'$ and (m, m') is swap-blocking pair with $\Phi(m) = k, \Phi(m') = k' \in \Phi$ **then**
- 25: $\Phi \leftarrow \Phi_{mk}^{m'k'}, x_{ms'} = x_{m's} = 1, x_{ms} = x_{m's'} = 0$;
- 26: **end if**
- 27: **end for**
- 28: **end for**
- 29: **until** there is no swap-blocking pairs existed in Φ
- 30: Find the best number of BS users num_B with $\min_{m \in \mathcal{U}^R} t_m(\lambda_m^{opt}, \lambda_m^{opt} \in (\lambda_m^{optR}, \lambda_m^{optB}))$;
- 31: Update $f_m^{optR} = \frac{f^R}{|\mathcal{U}^R| - num_B}, f_m^{optB} = \frac{f^B}{num_B}$;
- 32: **for** $m \in \mathcal{U}^R$ **do**
- 33: $\Delta t_m = t_m(\lambda_m^{optR}) - t_m(\lambda_m^{optB})$;
- 34: **if** $\Delta t_m > 0$ && $E_m^{eR} > E_m^{eB}$ **then**
- 35: $\mathcal{U}^R \setminus m, \mathcal{U}^B \cup m$;
- 36: **end if**
- 37: **end for**
- 38: **if** $|\mathcal{U}^B| > num_B$ **then**
- 39: Remove the user with the smallest Δt_m in \mathcal{U}^B to \mathcal{U}^R until $|\mathcal{U}^B| = num_B$;
- 40: **else if** $|\mathcal{U}^B| < num_B$ **then**
- 41: Add $m' \in \mathcal{U}^R$ to \mathcal{U}^B until $|\mathcal{U}^B| = num_B, m'$ has the smallest $t_m(\lambda_m^{optB})$ among \mathcal{U}^R with $\Delta t_m \geq 0$;
- 42: **if** $|\mathcal{U}^B| < num_B$ **then**
- 43: Add $m'' \in \mathcal{U}^R$ to \mathcal{U}^B until $|\mathcal{U}^B| = num_B, m''$ has the biggest Δt_m among \mathcal{U}^R with $\Delta t_m < 0$;
- 44: **end if**
- 45: **end if**

and BS users. We also take into account the case of resource deficit. In Step 12, the user still prefers the sub-channel s with the best transmission performance, but will compete with

user m_1 that previously obtained the sub-channel. Considering the optimization objective, the user with a greater difference between the delay of fully remote execution and that of fully local execution has a higher privilege in accessing resource s . The criterion in Step 13 not only requires user m to satisfy the sufficient and necessary conditions for offloading (see Step 8), but also has a higher privilege than the previously matched user m_1 . In this case, user m is accepted, user m_1 is rejected, and we have $\Phi = \Phi \setminus (m_1, k) \cup (m, k)$.

So far, the algorithm has determined which users can be served and makes the initial sub-channel allocation close to the optimization goal, thus reducing the complexity of the subsequent matching game. All the served users are temporarily associated with the MR. After determining the best user-sub-channel matching through the matching game in Steps 20-29, the algorithm then decides for each user whether to be associated with the MR or the BS depending on its best sub-channel in Steps 30-45.

The set \mathcal{U}^R sorts out all users that need to partially offload their tasks. From Steps 20-29, in one iteration, the algorithm first obtains λ_m^{optR} and f_m^{opt} for each $m \in \mathcal{U}^R$. Based on these values, all user pairs are examined to find the candidate swap-blocking pair. Then swap matching is triggered, and resource allocation changes dynamically as the matching game evolves. The condition under which the alternating iteration is ended is that $|\mathcal{U}^R| * (|\mathcal{U}^R| - 1)$ user pairs are not swap-blocking pairs.

In Step 30, the algorithm changes the number of users associated with the BS in \mathcal{U}^R , to find the optimal num_B that minimizes the total delay. After obtaining the optimal num_B , Steps 31-45 determine which users should be associated with the BS. First, according to the optimal num_B , the optimal BS and MR CPU frequencies for each user are obtained in Step 31. Then the latency of the respective MR association and BS association for each user is derived, whose difference is recorded at Δt_m . In Steps 32-37, the algorithm selecting the BS users for \mathcal{U}^B according to the time delay and energy consumption. These two metrics are better for users in \mathcal{U}^B than they would be if they were associated with MR. Note that, considering the energy consumption constraints of the MR, the energy consumption of the BS users is related to wireless transmission, while that of the MR users is related to the calculation in (8). The number of BS users selected in the above steps is not necessarily equal to the optimal num_B . If it is larger than the optimal num_B , the algorithm changes the associations of those users whose latency will be affected slightly by this change in Step 39. Otherwise, we need to add some users from \mathcal{U}^R to \mathcal{U}^B . Each time the user is selected who has the lowest latency if associated with the BS and $\Delta t_m > 0$, until the optimal num_B is reached. Here $\Delta t_m > 0$ indicates that it is better for the user to choose the BS than the MR in terms of delay. If all the users with $\Delta t_m > 0$ have been selected but we still have $|\mathcal{U}^B| < num_B$, then the users with $\Delta t_m < 0$ will be selected. These users actually prefer to be associated with the MR. Thus, we choose users with a small difference in delay between these two types of associations, while the biggest Δt_m indicates the smallest difference in delay in these two cases.

The computational complexity of Algorithm 1 mainly

comes from three parts. First, from Steps 2-18, most computations are from Step 3 and Step 12 for each user, with complexity $O(MS)$. The second part comes from Steps 20-29, where each iteration takes $O(|\mathcal{U}^R|^2)$ to determine all the swap-blocking pairs. We assume the algorithm converges after I iterations. Then the complexity is $O(I|\mathcal{U}^R|^2)$. Finally, in Steps 30-45, It takes $O(\log_2 |\mathcal{U}^R|)$ iterations to find num_B using binary search in Step 30, and $O(|\mathcal{U}^R|)$ to determine the association. Thus, the computational complexity of the proposed algorithm is $O(MS + I|\mathcal{U}^R|^2)$ for $|\mathcal{U}^R| < M$.

B. MR Energy Constraint Algorithm

The proposed RACO algorithm does not consider the energy constraint of the MR. On the basis of the former algorithm, we need to ensure that the sum of the MR energy consumption of users does not exceed E^R in constraint (19n).

This problem can be transformed into a knapsack problem. The energy constraint of the MR is regarded as capacity of the knapsack, the MR energy consumed by each served user given by Algorithm 1 is equivalent to the weight of each item, and the partial offloading delay (t_m) is regarded as the value of the item. The smaller the delay, the higher the value. The problem to be solved here is, how to select the items to put in the knapsack, without violating the knapsack's capacity and maximize the total value. Specifically, we model the problem as a decimal knapsack problem, where a portion of an item can be selected and loaded into the knapsack, because it's easy to accomplish by reducing the offloaded data bits. Tasks for users who cannot fit into the knapsack will be executed locally.

The proposed Algorithm 2 consists of two parts. The first part is the greedy algorithm in Steps 4-14, and the second part is the heuristic algorithm in Steps 16-24. Finally, our optimization goal, minimizing the average delay of all users, will be achieved as the smaller one of the results of these two parts.

Specifically, we should first determine whether the total MR energy consumption of the served users given by Algorithm 1 exceeds E^R . If not, the result of Algorithm 1 will be the final optimal solution, and there is no need for executing this algorithm anymore. Otherwise, the rest of the algorithm in Steps 3-26 will be executed. In Step 3, the value rate of all service users was sorted from high to low and recorded in set \mathbf{U} , where the lower the delay per unit of energy consumption, the higher the rate. In Steps 4-6, users are put into the knapsack in the order of \mathbf{U} , until the remaining capacity cannot accommodate a user. Users that cannot be put into the knapsack will be put into \mathcal{U}^\times temporarily. Users who have been placed in the knapsack must be served. If there is still capacity left in the knapsack, the next steps in Lines 8-25 will be executed to reduce the delay of all users as much as possible. Otherwise, all the rejected users in \mathcal{U}^\times will not perform partial offloading and their tasks will be executed locally. In Steps 8-14, the remaining knapsack capacity is first used to load the first user in \mathcal{U}^\times (i.e. user k), because the user has the highest rate. As mentioned above, only a part of user k 's task can be fitted into the knapsack, which means that measures need to be taken to reduce the MR energy consumption for this user to $(E^R - E)$.

Algorithm 2 The MR Energy Constraint Algorithm

Input: \mathcal{U}^R and \mathcal{U}^B
Output: $\bar{t} = \frac{1}{M} \sum_{m=1}^M t_m, m \in \mathbf{M}$
1: E = the total MR energy of all users in \mathcal{U}^R and \mathcal{U}^B ;
2: **if** $E > E^R$ **then**
3: \mathbf{U} = user set in ascending order of $\frac{t_m}{E_m^{eR}}, E_m^{eR} \in \{E_m^{eR}, E_m^{tR}\}$;
4: **for** $m \in \mathbf{U}$ **do**
5: Update $\mathcal{U}^R, \mathcal{U}^B$ and \mathcal{U}^\times , where $E \leq E^R, E + E_k^{eR} > E^R$, and k is the first user in \mathcal{U}^\times ;
6: **end for**
7: **if** $E^R - E > 0$ **then**
8: **if** k is a MR user **then**
9: **repeat**
10: Update $f_k^R = \sqrt{\frac{E^R - E}{\xi(1 - \lambda_k^R) d_k c_k}}, \lambda_k^R, \mathcal{U}^R, E_k^{eR}$;
11: **until** $0 \leq E^R - (E + E_k^{eR}) \leq \varepsilon_1$
12: **else if** k is a BS user **then**
13: Update $\lambda_k^B = 1 - \frac{(E^R - E) R_{k,s}^B}{P_k^R d_k}, t_k(\lambda_k^B), \mathcal{U}^B$;
14: **end if**
15: Calculate $T_1 = \sum t_m, m \in \mathbf{M}$;
16: **if** \mathcal{U}^\times contains MR users **then**
17: **repeat**
18: $\mathcal{U}^\times \setminus m', \mathcal{U}^R \cup m', m'$ is the 1th user in \mathcal{U}^\times ;
19: **while** $E^R - E < 0$ **do**
20: $f_n^R = f_n^R - \varepsilon_2$, update $\lambda_n^R, t_n, n \in \mathcal{U}^R$;
21: Calculate $T_2 = \sum t_m, m \in \mathbf{M}$;
22: **end while**
23: **until** T_2 is no longer decreasing or no MR user in \mathcal{U}^\times
24: **end if**
25: $\bar{t} = \frac{1}{M} \min\{T_1, T_2\}$;
26: **end if**
27: **end if**

If user k is associated with the MR, we can keep E_k^{eR} within the constraint by reducing f_k^R according to (8). As f_k^R is decreased, the offloaded fraction of the task will be adjusted accordingly; f_k^R and λ_k^R interact with each other iteratively, so that E_k^{eR} converges to E^R . If user k is associated with the BS, we can keep the E_k^{tR} within the constraint by reducing the offloaded fraction (i.e. $1 - \lambda_k^B$) according to (14) and (16). Finally, all users in \mathcal{U}^\times except k are denied service, and all their tasks will be executed locally.

In Steps 16-24, we use another strategy to constrain the MR energy consumption of served users. According to (8), decreasing f_m^R linearly will reduce E_m^{eR} exponentially. Thus, we appropriately reduce f_m^R of users in \mathcal{U}^R obtained in Step 5, leaving more MR energy to serve the MR users in \mathcal{U}^\times . That is to say, the latency of the users in \mathcal{U}^R will be sacrificed for reducing the total delay. This is because the computing capacity of the MR is far better than that of the local device. In Steps 17-23, the number of served MR users is gradually increased, and the f_m^R of the users in the set is adjusted uniformly every time \mathcal{U}^R is updated. When the total delay of users cannot be further reduced or when there is no MR user in \mathcal{U}^\times , we stop the iteration. In Steps 19-22, f_m^R is adjusted by setting a reasonable step size, and the optimal offloaded fraction of each MR user is updated according to (27), until the total MR energy consumption of served users becomes lower than E^R . Finally, Step 25 indicates that the solution to problem **P1** is obtained by comparing the outcomes of the two

TABLE II
SIMULATION PARAMETERS

| Parameter | Symbol | Value |
|--------------------------------|-----------------|--------------------------|
| Noise spectral density | N_0 | -134 dBm/MHz |
| User transmit power | P_m | 5 dBm |
| Path loss exponent | α | 3 |
| SI cancelation level | β | $10^{-12} \sim 10^{-11}$ |
| Half-power beamwidth | θ_{-3dB} | 30° |
| Effective switched capacitance | μ | 5×10^{-27} |
| Energy accuracy | ε_1 | 0.001 J |
| Frequency accuracy | ε_2 | 0.002 GHz |

schemes in Algorithm 2.

The computation complexity of Algorithm 2 mainly lies in the iterative Steps 9-11 and 17-23. In Steps 17-23, the outer loop is executed at most $|U^\times|$ times. For the inner loop, the number of iterations of the *while* loop is determined by the accuracy tolerance ε_2 . Given $\varepsilon_2 > 0$, the complexity of the one dimensional search on f_m^R is $O(\log(1/\varepsilon_2))$.

VII. PERFORMANCE EVALUATION

A. Simulation Setup

In this section, we evaluate the performance of the proposed schemes by comparing with several baseline schemes, and the simulations are conducted in MATLAB. In the simulation scenario, Multiple users are scattered in a circular area centered at the MR with a radius of 120m, and a BS is 500m away from the MR. Different local device applications can be distinguished by the size of computing data d_m , which follows a uniform distribution between [1,4]Mbits. The computation workload c_m follows the uniform distribution between [300,500]cycles/bit. The maximum local computation capacity f_m^{max} follows the uniform distribution between [0.3,0.5]GHz. The local energy constraint E_m for each user is randomly chosen between $\{0.5, 1.2, 1.8\}J$. unless otherwise specified, the MR and BS computation capacity f^R and f^B are set to 8GHz and 24GHz, respectively. The mmWave frequency band used in the simulations is 28GHz and the bandwidth is 2GHz. In addition, the channel follows the Nakagami distribution with parameters $m_s = 3$ and $w_s = \frac{1}{3}$ [22] and the mm-wave realistic directional antenna model from IEEE 802.15.3c [27]. Other parameter settings are provided in Table II. The results of simulation studies in this section are based on an average over a number of Monte Carlo simulations for various system parameters. The benchmark schemes are as follows.

- **USRA**: When determining the served users, the order of users accessing sub-channel resources is random. The served users still determine the optimal sub-channel through the matching game, but it is random for users to associate with the MR or the BS on their optimal sub-channel. In addition, only the first part of Algorithm 2 is used for enforcing the MR energy consumption constraint.
- **RUNP**: Select the served users randomly according to the number of sub-channels. For those users associated with the BS, the transmit power for the MR, P_m^R , is randomly

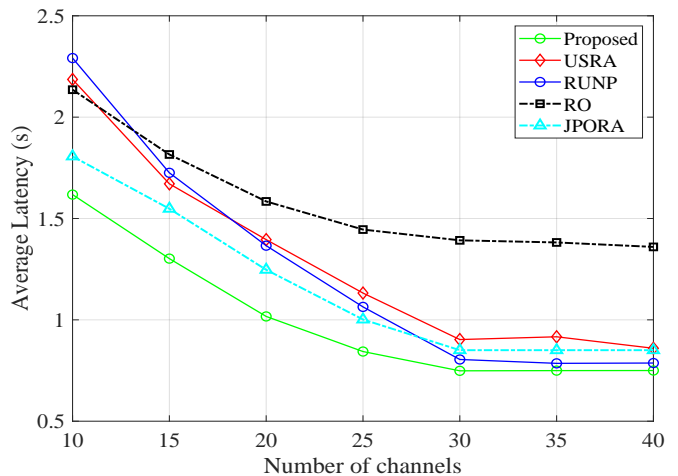


Fig. 3. Average latency of the four schemes with different numbers of sub-channels.

selected from $[0.1, 0.6] W$. The remaining parts are the same as that in our scheme.

- **RO**: The fraction of task data to be offloaded for each served user is decided randomly, while user association and matching game are the same as that in our scheme. Only the first part of Algorithm 2 is used for enforcing the MR energy consumption constraint.
- **JPORA**: Similar to the existing work in [23], the user association problem is solved based on the location of users, users within the BS coverage radius are associated with it. Subcarrier assignment of a user based on maximum marginal data rate. Optimizing offloading ratio iteratively, iteration ends when the average local computation delay and average computation offloading delay of all users are equal.

In Table III, IV, we give 95% confidence interval with the normal distribution analysis of several random algorithms in Fig. 3 and Fig. 4, where mu is the mean and sigma is the standard deviation.

B. Comparison with Baseline Schemes

As communication resource allocation is a challenging part of the problem, we need to determine the available sub-channels to verify the application of our scheme in practical scenarios. In Fig. 3, the numbers of users are set to 30. When resources are insufficient, that is, the number of sub-channels varies from 10 to 25, all the four schemes enable more users to take advantage of the parallelism by partitioning and offloading part of the tasks to edge computing. The average latency is observed to decrease with increased number of channels. The similar performance of USRA and RUNP shows that sometimes communication resource matching is superior to computation resource allocation, and sometimes vice versa. Although RO has the worst performance in most cases, it can even outperform USRA and RUNP when communication resources are scarce, with a well-chosen set of users. When the number of sub-channels exceeds 25, all users have the opportunity to offload their tasks, and the average latency

TABLE III
CONFIDENCE INTERVAL ANALYSIS OF DIFFERENT NUMBER OF CHANNELS

| Number of channels | USRA | | RUNP | | RO | |
|--------------------|-----------------|-----------------|-----------------|-----------------|-----------------|-----------------|
| | mu | sigma | mu | sigma | mu | sigma |
| 10 | [2.1667,2.2109] | [0.0976,0.1292] | [2.2829,2.3042] | [0.0472,0.0625] | [2.1237,2.1496] | [0.0572,0.0756] |
| 15 | [1.6467,1.6878] | [0.0910,0.1203] | [1.7180,1.7397] | [0.0482,0.0637] | [1.8005,1.8242] | [0.0523,0.0692] |
| 20 | [1.3720,1.4153] | [0.0958,0.1268] | [1.3469,1.3688] | [0.0484,0.0641] | [1.5662,1.5889] | [0.0503,0.0665] |
| 25 | [1.1864,1.2323] | [0.1015,0.1343] | [1.0825,1.1055] | [0.0509,0.0673] | [1.4270,1.4509] | [0.0529,0.0700] |
| 30 | [0.8895,0.9307] | [0.0912,0.1206] | [0.7871,0.7940] | [0.0150,0.0198] | [1.3717,1.3986] | [0.0596,0.0788] |
| 35 | [0.8683,0.9013] | [0.0729,0.0964] | [0.7839,0.7873] | [0.0075,0.0099] | [1.3669,1.3894] | [0.0496,0.0656] |
| 40 | [0.8732,0.9098] | [0.0811,0.1073] | [0.7835,0.7867] | [0.0072,0.0095] | [1.3416,1.3648] | [0.0513,0.0679] |

TABLE IV
CONFIDENCE INTERVAL ANALYSIS OF DIFFERENT NUMBER OF USERS

| Number of users | USRA | | RUNP | | RO | |
|-----------------|-----------------|-----------------|-----------------|-----------------|-----------------|-----------------|
| | mu | sigma | mu | sigma | mu | sigma |
| 15 | [0.6121,0.6493] | [0.0823,0.1089] | [0.3612,0.3666] | [0.0120,0.0159] | [1.2129,1.2358] | [0.0506,0.0669] |
| 20 | [0.6707,0.7060] | [0.0780,0.1032] | [0.3619,0.3677] | [0.0129,0.0170] | [1.2503,1.2734] | [0.0510,0.0675] |
| 25 | [0.6470,0.6833] | [0.0804,0.1064] | [0.4195,0.4271] | [0.0168,0.0223] | [1.2461,1.2680] | [0.0464,0.0649] |
| 30 | [0.7187,0.7445] | [0.0770,0.0954] | [0.5243,0.5427] | [0.0407,0.0538] | [1.3873,1.4102] | [0.0507,0.0671] |
| 35 | [1.0329,1.0659] | [0.0729,0.0964] | [0.7373,0.7577] | [0.0450,0.0596] | [1.4719,1.4953] | [0.0518,0.0685] |
| 40 | [1.2343,1.2653] | [0.0685,0.0907] | [0.9881,1.0106] | [0.0499,0.0660] | [1.6014,1.6231] | [0.0481,0.0637] |
| 45 | [1.6042,1.6372] | [0.0730,0.0965] | [1.3529,1.3750] | [0.0489,0.0647] | [1.9280,1.9511] | [0.0511,0.0677] |

tends to be roughly constant except for USRA. Because the random association may cause large amounts of users to be associated with the BS or the MR, and the resource allocated to each user is small, which makes the latency larger. Random assignment of some computing tasks to the edge server is clearly helpful to reduce the performance of RO compared with the proposed algorithm. Compared with RUNP, it is verified that the served user selection scheme in the proposed algorithm can effectively reduce the overall delay of all users. JPORA adjusts the offloading ratio uniformly for all users, resulting some users didn't get the optimal offloading ratio when the algorithm is stopped. According to the confidence interval, among the three random algorithms, RUNP is more stable when resources are surplus. While USRA has the highest uncertainty, indicating the importance of reasonable allocation of computation resources.

In Fig. 4, the number of sub-channels is set to 30 and the MR and BS computation capacity f^R and f^B are set to $12GHz$ and $36GHz$, respectively. The results of varying the number of users from 15 to 45 are obtained. With more users, resources will be more and more scarce, and a larger proportion of users can only complete the computing tasks through local execution, which causes the five curves to rise gradually. In addition, due to the disparity in computing capacity between local and edge servers, the latency of served users with RO is largely determined by the worse local latency, and thus, the performance is poor even when the resources are sufficient. Compared with RUNP and JPORA, with the full utilization of edge computing resources, power control and matching game also improves the system performance to a certain extent. JPORA is greatly affected by the location of users, so it cannot flexibly determine association relationships.

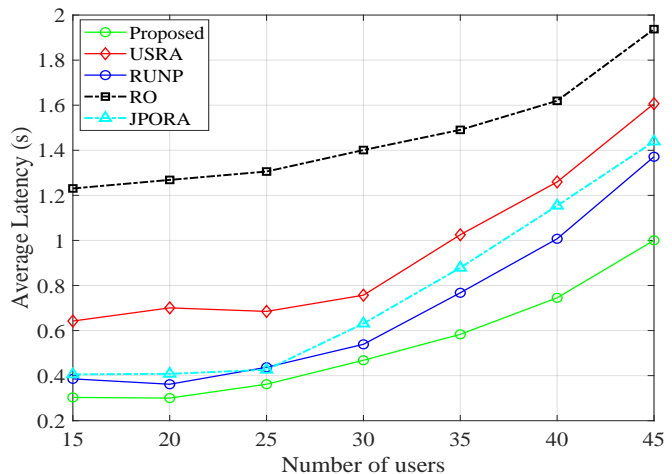


Fig. 4. Average latency of the four schemes with different numbers of users.

Similar to Table III, USRA has relatively large confidence interval at the same confidence level.

To examine the impact of different computation task sizes of diverse user applications, we verify the performance of the proposed algorithm by increasing the task size in Fig. 5. The number of sub-channels is set to 20 and the number of users is 30. Therefore, users compete for limited communication resources. For each data point, the task size is uniformly distributed between 1 Mbits and the task size value on that data point. Fig. 5 plots the average latency, and shows that it gradually increases with increased data size for all the schemes. This can be explained as, with the increase in task size, a higher fraction of data will be offloaded for remote

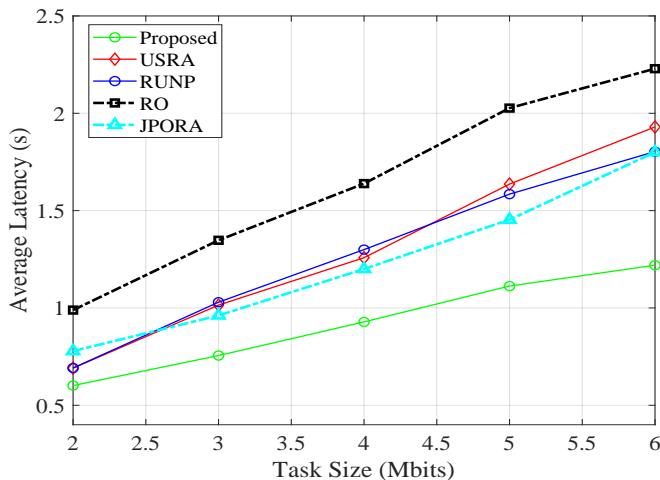


Fig. 5. Average latency of the four schemes with different task sizes.

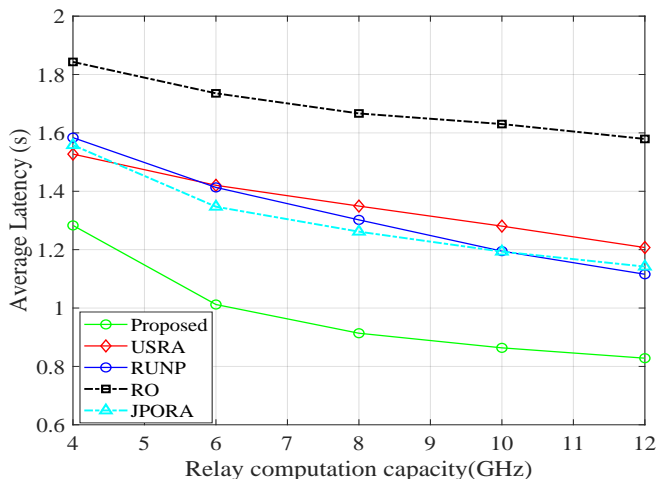


Fig. 6. Average latency of the four schemes with different MR computation capacities.

execution to overcome the limited computation capacity and local energy constraint at user devices, which in turn leads to higher transmission and computation delay. Furthermore, the remote execution time increases when the offloaded task size is increased. Our comparison study also shows that, the proposed scheme has the lowest increasing rate. Moreover, USRA, RUNP and JPORA have similar performance, it reduces the average latency by approximately 33% over USRA. These results show that our algorithm has advantages for computation intensive applications.

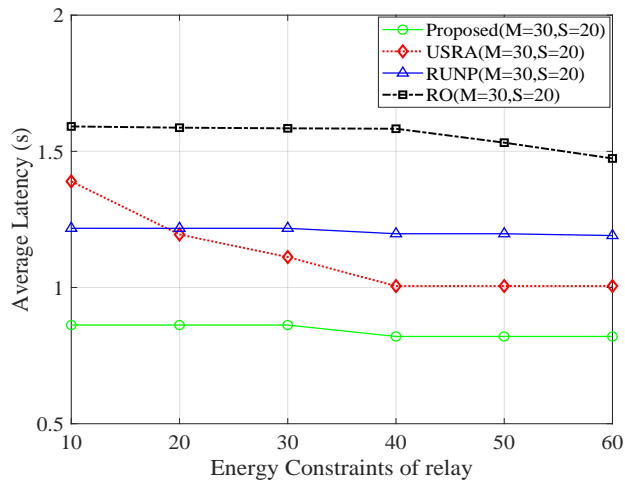
In order to analyze the impact of edge computation resources on the delay performance, we plot the average latency against computation capacity of the MR in Fig. 6, while maintaining the computing capacity of the BS as 3 times of the MR's computing capacity. The number of sub-channels is set to 20 and the number of users is 30. With the increase of computing resources, the average delay of all schemes exhibits a decreasing trend. The performance of the proposed algorithm is not significantly improved when the computing resources

exceeds a certain threshold, mainly because the delay of unserved users is too large that computing resources are no longer the primary constraint. For USRA, RUNP and JPORA, sometimes the benefit of computation resource allocation is better than that of optimizing the served set of users, and sometimes it is the opposite, which is why the intersection occurs. The proposed scheme achieves 35%, 32%, 50% and 31% lower latency than the other three baseline schemes in statistical average sense, respectively.

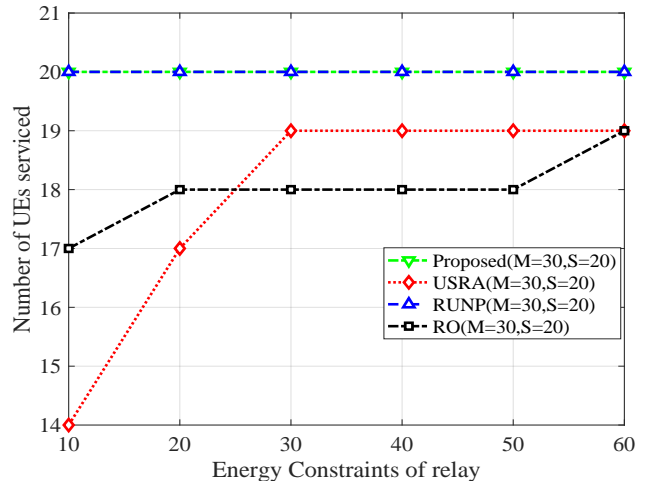
In Fig. 7, we provide a comparison of the average delay and the number of served users performance under different MR energy constraints. In addition, we examine two cases: (i) resource deficit in Fig. 7(a)(b) with 30 Users and 20 Sub-channels, and (ii) resource surplus in Fig. 7(c)(d) with 20 Users and 25 Sub-channels. It is obvious that no matter it is resource deficit or resource surplus, RUNP and the proposed scheme that use Algorithm 2 are basically stable in terms of average delay, while the delay of USRA and RO using the greedy algorithm (i.e., the first part of Algorithm 2) decreases with the relaxation of the constraint. However, the performance does not improve any further beyond a certain threshold as the MR energy does not remain the dominant constraint. In addition, RUNP and the proposed scheme also serve more users than USRA and RO under the same conditions. The proposed algorithm is better than the other algorithms in both the latency and the number of served users, especially when the resources are insufficient where there are users competing for resources.

VIII. CONCLUSION AND FUTURE WORK

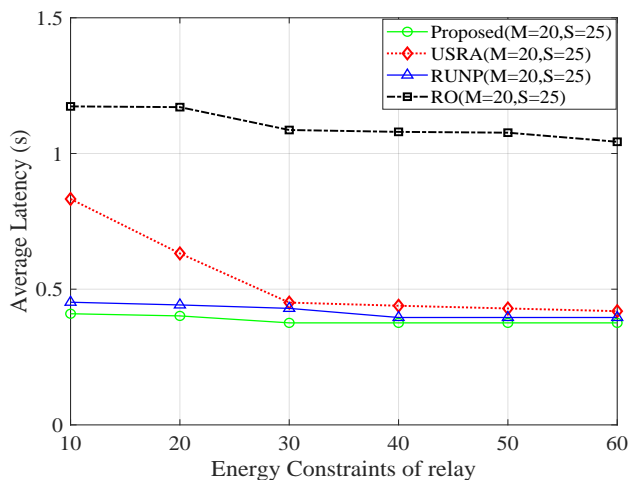
In this paper, we investigated the problem of user association, resource allocation (including communication and computation resources), and computation offloading in the uplink train-ground communication scenario. In terms of minimizing the parallel computing latency under MR energy consumption control, we decomposed the optimization problem into three sub-problems for ease of analysis. The continuous variables, including the local device computational speed, offloading ratio, and transmit power of the MR were obtained through functional analysis. Efficient resource allocation was implemented as binary variable determined by a dynamic matching game. The RACO algorithm was proposed to solve the sub-problems alternately, to obtain suboptimal solutions. Then a heuristic MR energy consumption control algorithm was proposed to finally adjust the offloading rate and MR calculation frequency assigned to the served users, in order to enforce the MR energy consumption constraint. Through extensive simulations under different network parameters, we demonstrated the superiority of the proposed scheme over three baseline schemes. The proposed algorithm is suitable for computation offloading scenarios where the energy consumption and computing resources of edge servers are limited, but only consider the task can be completed when the users shift from the connecting BS to another adjacent BS. Future work is to investigate the blockage problem and cooperative D2D communications in the proposed framework.



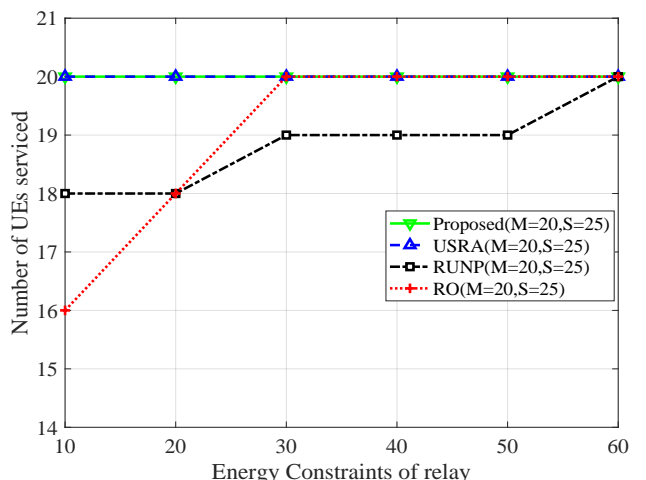
(a) Resource deficit: 30 Users and 20 Sub-channels



(b) Resource deficit: 30 Users, and 20 Sub-channels



(c) Resource surplus with 20 Users and 25 Sub-channels



(d) Resource surplus with 20 Users and 25 Sub-channels

Fig. 7. Average latency and the number of served users of the four schemes with different MR energy constraints.

REFERENCES

- [1] B. Ai et al., "Challenges Toward Wireless Communications for High-Speed Railway," in *IEEE Transactions on Intelligent Transportation Systems*, vol. 15, no. 5, pp. 2143-2158, Oct. 2014, doi: 10.1109/TITS.2014.2310771.
- [2] M. Elkashlan, T.Q. Duong, and H.-H. Chen, "Millimeter-wave communications for 5G: fundamentals:Part I [Guest Editorial]," *IEEE Communications Magazine*, vol. 52, no. 9, pp. 52-54, Sept. 2014.
- [3] 3GPP, "Study on New Radio (NR) Access Technology-Physical Layer Aspects," *TR 38.802 (Rel. 14)*, 2017.
- [4] C. Han and S. Duan, "Impact of atmospheric parameters on the propagated signal power of millimeter-wave bands based on real measurement data," *IEEE Access*, vol. 7, pp. 113626-113641, Aug. 2019.
- [5] Y. Niu, Y. Li, D. Jin, L. Su, and D. O. Wu, "Blockage robust and efficient scheduling for directional mmWave WPANs," *IEEE Transactions on Vehicular Technology*, vol.64, no.2, pp.728-742, Feb. 2015.
- [6] W. Gheth, K.M. Rabie, B. Adebisi, M. Ijaz, and G. Harris, "Communication systems of high-speed railway: A survey," *Trans. Emerging. Tel. Tech.*, vol.32, pp.e4189, 2021.
- [7] M. Heino, et al., "Recent advances in antenna design and interference cancellation algorithms for in-band full duplex relays," *IEEE Commun. Mag.*, vol.53, no.5, pp.91-101, May 2015.
- [8] V. Tapio, M. Sonkki, and M. Juntti, "Self-interference cancellation in the presence of non-linear power amplifier and receiver IQ imbalance," *J. Wireless Commun. Netw.*, Article number: 127, June 2020.
- [9] W.G. Ding, Y. Niu, H. Wu, Y. Li, and Z.D. Zhong, "QoS-aware full-duplex concurrent scheduling for millimeter wave wireless backhaul networks," *IEEE Access*, vol.6, pp.25313-25322, 2018.
- [10] J. Liu, Y. Mao, J. Zhang, and K.B. Letaief, "Delay-optimal computation task scheduling for mobile-edge computing systems," in *Proc. IEEE Int. Symp. Inf. Theory (ISIT'16)*, Barcelona, Spain, July 2016, pp.1451-1455.
- [11] Y. Wang, M. Sheng, X. Wang, L. Wang, and J. Li, "Mobile-edge computing: Partial computation offloading using dynamic voltage scaling," *IEEE Trans. Commun.*, vol.64, no.10, pp.4268-4282, Oct. 2016.
- [12] Z. Zhao, S. Bu, T. Zhao, Z. Yin, M. Peng, Z. Ding, and T.Q.S. Quek, "On the design of computation offloading in fog radio access networks," *IEEE Trans. Veh. Technol.*, vol.68, no.7, pp.7136-7149, July 2019.
- [13] D.Z. Wen and G.D. Yu, "Time-division cellular networks with full-duplex base stations," *IEEE Commun. Lett.*, vol.20, no.2, pp.392-395, Feb. 2016.
- [14] W.G. Ding, Y. Niu, H. Wu, Y. Li, and Z.D. Zhong, "QoS-aware full-duplex concurrent scheduling for millimeter wave wireless backhaul networks," *IEEE Access*, vol.6, pp.25313-25322, May. 2018.
- [15] M. Liu, Y. Mao, S. Leng, and S. Mao, "Full-duplex aided user virtualization for mobile edge computing in 5G networks," *IEEE Access*, vol.6, pp.2996-3007, 2018.
- [16] Y. Lan, X. Wang, D. Wang, Y. Zhang, and W. Wang, "Mobile-edge computation offloading and resource allocation in heterogeneous wireless networks," in *Proc. IEEE WCNC'19*, Marrakech, Morocco, Apr. 2019, pp.1-6.
- [17] Z. Ning, P. Dong, X. Kong, and F. Xia, "A cooperative partial computation offloading scheme for mobile edge computing enabled Internet

- of Things,” *IEEE Internet of Things J.*, vol.6, no.3, pp.4804–4814, June 2019.
- [18] Z. Kuang, L. Li, J. Gao, L. Zhao, and A. Liu, “Partial offloading scheduling and power allocation for mobile edge computing systems,” *IEEE Internet of Things J.*, vol.6, no.4, pp.6774–6785, Aug. 2019.
- [19] H. Guo, J. Liu, and J. Zhang, “Efficient computation offloading for multi-access edge computing in 5G HetNets,” in *Proc. IEEE ICC’18*, Kansas City, KS, May 2018, pp.1–6.
- [20] Y. Mao, J. Zhang, S.H. Song, and K.B. Letaief, “Stochastic joint radio and computational resource management for multi-user mobile-edge computing systems,” *IEEE Trans. Wireless Commun.*, vol.16, no.9, pp.5994–6009, Sept. 2017.
- [21] U. Saleem, Y. Liu, S. Jangsher, and Y. Li, “Performance guaranteed partial offloading for mobile edge computing,” in *Proc. IEEE GLOBE-COM’18*, Abu Dhabi, United Arab Emirates, pp.1–6.
- [22] Y. Chen, B. Ai, Y. Niu, et al., “Energy efficient resource allocation and computation offloading in millimeter-wave based fog radio access Nnetworks,” in *Proc. IEEE ICC’20*, Virtual Conference, June 2020, pp.1–7.
- [23] U. Saleem, Y. Liu, S. Jangsher, et al., “Latency minimization for D2D-enabled partial computation offloading in mobile edge computing,” *IEEE Trans. Veh. Technol.*, vol.69, no.4, pp.4472–4486, Apr. 2020.
- [24] E. Meskar, T.D. Todd, D. Zhao, and G. Karakostas, “Energy aware offloading for competing users on a shared communication channel,” *IEEE Trans. Mobile Comput.*, vol.16, no.1, pp.87–96, Jan. 2017.
- [25] H. Guo and J. Liu, “Collaborative computation offloading for multi-access edge computing over fiber-wireless networks,” *IEEE Trans. Veh. Technol.*, vol.67, no.5, pp.4514–4526, May 2018.
- [26] B. Di, L. Song, and Y. Li, “Sub-channel assignment, power allocation, and user scheduling for non-orthogonal multiple access networks,” *IEEE Trans. Wireless Commun.*, vol.15, no.11, pp.4268–4282, Oct. 2016.
- [27] IEEE 802.15 WPAN Millimeter Wave Alternative PHY Task Group 3c (TG3c), “Wireless Medium Access Control (MAC) and Physical Layer (PHY) specifications for high rate Wireless Personal Area Networks (WPANs) (Amendment 2: Millimeter-wave-based Alternative Physical Layer Extension),” Oct. 2009.
- [28] Y. Zhu, Y. Niu, J. Li, D.O. Wu, Y. Li, and D. Jin, “QoS-aware scheduling for small cell millimeter wave mesh backhaul,” in *Proc. IEEE ICC’16*, Kuala Lumpur, Malaysia, May 2016.
- [29] L. X. Cai, L. Cai, X. Shen, and J.W. Mark, “Rex: A randomized exclusive region based scheduling scheme for mmWave WPANs with directional antenna,” *IEEE Trans. Wireless Commun.*, vol.9, no.1, pp. 113–121, Jan. 2010.
- [30] Y. Mao, C. You, J. Zhang, K. Huang, and K.B. Letaief, “A survey on mobile edge computing: The communication perspective,” *IEEE Commun. Sur. Tut.*, vol.19, no.4, pp.2322–2358, Fourthquarter 2017.
- [31] O. Munoz, A.P. Iserte, and J. Vidal, “Optimization of radio and computational resources for energy efficiency in latency-constrained application offloading,” *IEEE Trans. Veh. Technol.*, vol.64, no.10, pp.4738–4755, Oct. 2014.
- [32] Y. Chen, B. Ai, Y. Niu, K. Guan, and Z. Han, Resource Allocation for Device-to-Device Communications Underlying Heterogeneous Cellular Networks Using Coalitional Games, *IEEE Transactions on Wireless Communications*, vol. 17, no. 6, pp. 4163C4176, Jun. 2018.
- [33] L. Chen, F.R. Yu, H. Ji, G. Liu, and V.C.M. Leung, “Distributed virtual resource allocation in small-cell networks with full-duplex selfbackhails and virtualization,” *IEEE Trans. Veh. Technol.*, vol.65, no.7, pp.5410–5423, July 2016.